JOURNAL OF MATERIALS SCIENCE **36** (2001) 3785–3792

The effect of processing on the properties of poly(3-hydroxybutyrate-co-3-hydroxyvalerate) copolymers

R. CHAMBERS, J. H. DALY*, D. HAYWARD, J. J. LIGGAT
Department of Pure and Applied Chemistry, University of Strathclyde, Glasgow G1 1XL, Scotland
E-mail: j.h.daly@strath.ac.uk

Semi-crystalline poly(3-hydroxybutyrate-co-3-hydroxyvalerate) copolymers are biodegradable systems with potential as substrates for use in tissue regeneration. Previous studies have shown that severe embrittlement occurs on storage at room temperature restricting their application possibilities. Concepts such as secondary, advancing crystallisation causing changes in the amorphous/crystalline ratio have been mooted as the cause of the embrittlement. Using films prepared by extrusion and compression moulding procedures we have attempted to probe not only the pure amorphous and crystalline phases but also the interfacial region. Interpretation of dynamic mechanical and dielectric data highlights the changes in the nature of the interfacial region on processing. Moreover, the use of the Thermally Stimulated Discharge technique is a powerful probe for highlighting the morphological changes induced in multiphase systems by the processing step.

1. Introduction

There is great interest in polyhydroxyalkonates as biodegradable polymers [1] in medical applications, exploiting the key features of biocompatibility and biodegradation over timescales appropriate to tissue regeneration. The class includes the 3-hydroxybutyrate-co-3-hydroxyvalerate (HB/HV) copolymers marketed under the Biopol trademark (Fig. 1).

These copolymers are semi-crystalline with melting temperature ranging from 120°C to 180°C depending on the composition. Flexibilty and ductility improves with increasing hydroxyvalerate content. Extensive studies of the crystallisation behaviour of these polymers has shown that both monomer units have very similar crystal lattice requirements and exhibit the phenomenon of isodimorphism.

The main disadvantage of these materials, however, is their ability to undergo an ageing process on storage which results in severe embrittlement. This process, reminiscent of physical ageing, has been attributed to the development of a secondary, advancing crystallisation and a progressive reduction of the amorphous content in the partially crystalline polymer [2–4]. Subsequent annealing of samples was shown to rejuvenate the properties of the material. A change in the lamellar morphology, which reduces the amorphous-crystalline interface area and thus the constraint imposed on the amorphous chains by the crystals, is hypothesised to explain the observations [3].

The characterisation of Biopol^{TM} systems has been made using a plethora of methods, including e.g. Differential Scanning Calorimetry (DSC), Dynamic Mechanical Thermal Analysis (DMTA), Dielectric techniques [5–7] and ultimate mechanical properties such as tensile strength, modulus and elongation. Although each in its own right is very useful, it should be stated that they tend to uniquely highlight the amorphous or crystalline phase. For example, DSC gives data which biases the crystalline phase by monitoring the melting point and degree of crystallinity. The nature of the amorphous component is best served by DMTA and dielectric techniques. The characteristics of the interfacial region, however, are much more difficult to observe. The dielectric work of Pratt and Smith [5] is the exception in that they have identified a process consistent with a polarisation at the crystalline-amorphous interface. The studies to date, especially with respect to dielectric examination, are limited and tended to look at the homopolymer moiety under one specific processing condition.

In this study we have carried out an extensive examination of two HB/HV copolymers prepared by both film extrusion and compression moulding techniques. In addition to DSC, DMTA and dielectric spectroscopy we present the first recorded data of the systems being investigated using Thermally Stimulated Discharge Currents (TSD) [8]. This technique will be used to examine the effects of polymer processing, and, together

* Author to whom correspondence should be addressed.

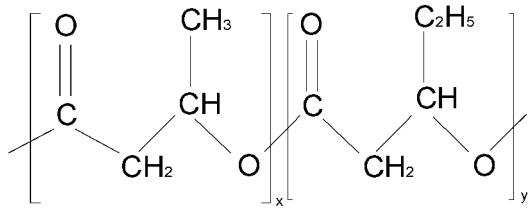

3-hydroxybutyrate-co-3-hydroxyvalerate

Figure 1 Structure of Biopol™ copolymers.

with additional dielectric analysis, will serve to show that examination of the crystalline-amorphous region is possible.

2. Experimental

Two grades of Biopol™ biodegradable polyester copolymers containing 8% (D400G) and 12% (D600G) of hydroxyvalerate component were obtained from Monsanto plc. Both grades contain 1% of boron nitride as a nucleating agent. The materials were processed as films using a Prism TSE-16-TC twin screw extruder with a cast film die. Processing conditions in the extruder ranged from 150°C to 160°C for the D400G system, and 150°C to 155°C for the D600G material. The films were formed using a temperature controlled haul-off system; for both materials the temperature of the rollers was constant at 65°C. Compression moulded pieces were fabricated under pressure between glass plates at 165°C (D400G) and 160°C (D600G). The samples were cooled slowly (ca. 30 minutes) under pressure to room temperature prior to removal from the glass plates.

Differential Scanning Calorimetry (DSC) was used to assess the crystallinity of the films. Analyses were carried out using a Du Pont 910 DSC coupled with the Du Pont 990 programmer/recorder. The samples were placed in sealed pans under nitrogen, and scans in the temperature range of 40°C to 200°C were carried out at the rate of 10°C/minute. Indium was used as a calibration standard.

DMTA was carried out using a Polymer Laboratories Mark III apparatus. Scans of E′ and E″ were obtained at 1 Hz using a heating rate of 3°C/minute.

The dielectric properties were obtained from 10^{-2} Hz to 65 kHz using the apparatus described previously [9]. Electrodes (gold/palladium) were evaporated onto the samples using an Edwards High Vacuum coating facility. The Thermally Stimulated Discharge (TSD) experiments were carried out using a Source Measure Unit (SMU type 237, Keithley Instruments) whose current sensitivity capabilities are equal to those of an electrometer. This device is capable of providing both the d.c.voltage (programmable upto 1100 V) and the measured discharge current (as low as 10^{-14} A). The dielectric cell and environmental chamber used was the same as for the dielectric measurements. [Unless otherwise stated, the samples were examined within 1 day of preparation].

3. Results and discussion

3.1. Differential scanning calorimetry (DSC)

As has been previously observed [10] more than one melting endotherm can be observed in Biopol systems. We observed that for the extruded systems (both D400G and D600G) bimodal endotherms are in evidence (Fig. 2). For the compression moulded pieces a single endotherm is observed. These multiple endotherms have been rationalised in terms of e.g.; heterogeneous distribution of crystal compositions, distinct pre-existing crystalline morphologies and the melting of thin, unstable crystals.

The difference in the nature of the endotherms for extruded and compression moulded parts can be explained in terms of the inherent thermal history. In the case of the compression moulded materials (one endotherm) the slow cooling from the melt gives ample time for the crystalline structure to form to produce a homogeneous crystalline phase. For the extruded systems, there is an element of 'quenching' in that on exit from the cast film die the material drops suddenly in temperature before being drawn through the haul-off rollers. This thermal history is sufficient to thus produce a crystalline morphology with a degree of inhomogeneity. The most significant observation, however, is that the overall crystallinity parameters (Table I) in respect of melt endotherm and calculated crystallinity [11] are not significantly affected by the processing conditions. This further highlights the hypothesis that changes in processing conditions affects the subtle texture of the crystalline morphology in terms of, such as, distribution of crystal composition and crystal thickness.

3.2. Dynamic mechanical thermal analysis (DMTA)

The DMTA data for the extruded and compression moulded D400G (8%HV) and D600G (12%HV) are

TABLE I DSC data for the compression moulded and extruded films

Sample	Processing	Remarks	Peak Endotherm (°C)	ΔH (J/g)	Crystallinity (%)
D400G	C.M.	Single melt	162	72.4	61
D400G	Extruded	Bimodal melt	153/161	71.8	61
D600G	C.M.	Single melt	152.5	59.6	53
D600G	Extruded	Bimodal melt	140/150	55.51	49.5

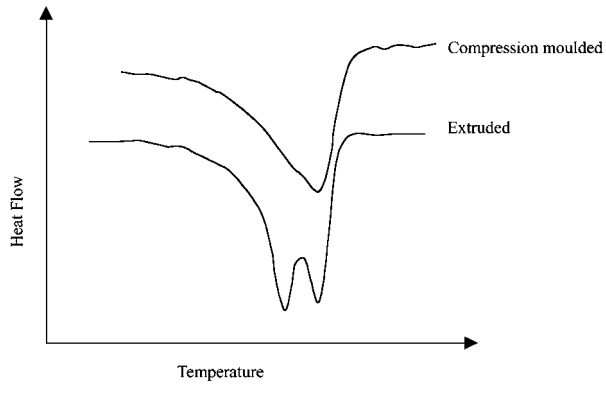

Figure 2 Characteristic DSC scans for compression moulded and extruded D600G (12% HV) copolymer.

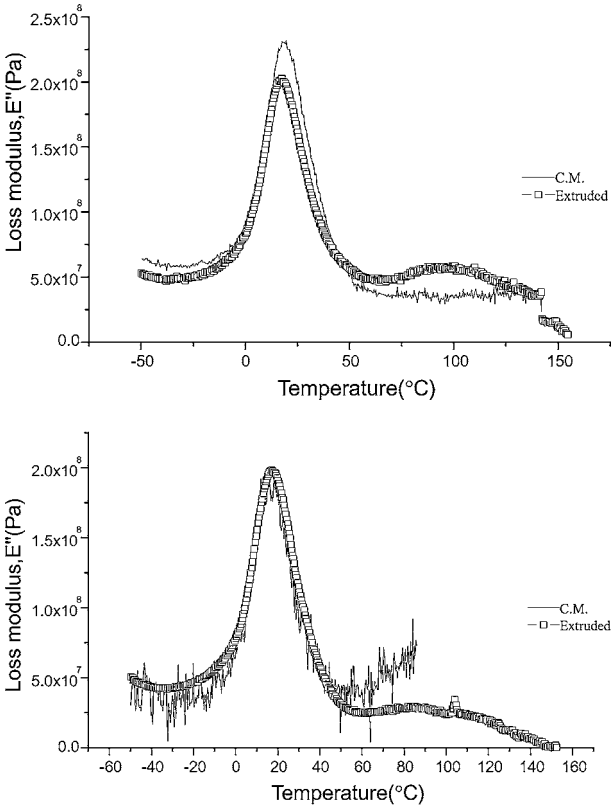

Figure 3 Loss modulus as a function of temperature for the compression moulded and extruded copolymers. [Top, D400G; Bottom, D600G]

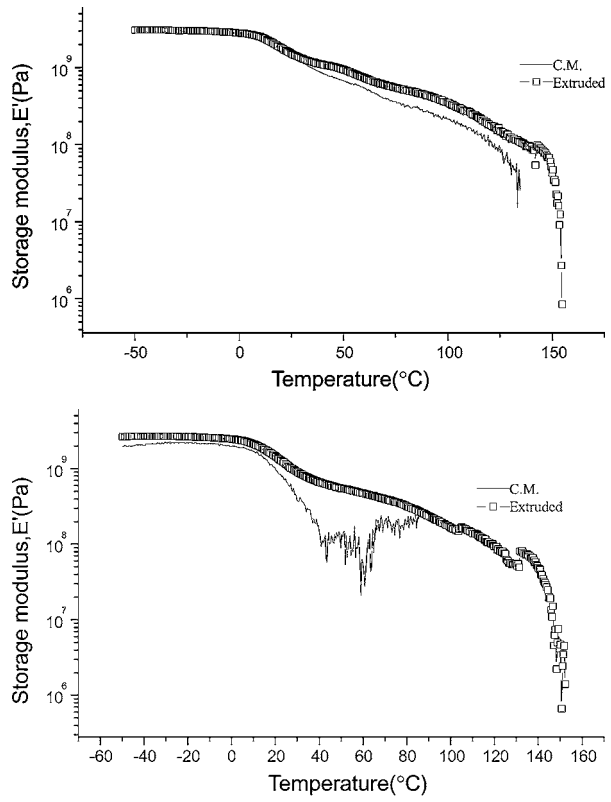

Figure 4 Storage modulus as a function of temperature for the compression and extruded copolymers. [Top, D400G; Bottom, D600G]

highlighted in Figs 3 and 4. From the E″ data we clearly observe a major transition around 20°C for all the samples. Furthermore, at higher temperatures we observe differences between the extruded and compression moulded parts. For both compositions the extruded material has a distinct feature occuring around 100°C. For the E′ data of Fig. 4 the differences are further exemplified. For the low HV level we see that the modulus falls off at slower rate for the extruded material. This observation is much more pronounced in the case of the higher HV system. The reason for this can be rationalised in terms of the morphology. For the compression moulded samples from the DSC data we have concluded that the slow cooling process results in a more homogeneous crystalline structure. We can infer that the amount of amorphous-crystalline interface will be affected. For the extruded material we may expect that the more rapid cooling will result in a more disordered amorphous-crystalline region. It is well known, from studies on polycarbonate/ABS blends [12–14], that in two-phased systems the degree of intermixing at the phase boundaries plays the major role in defining the ultimate mechanical properties. The connectivity between the phases, as well as the morphology of the components, defines the ability to transfer stress from one phase to the other during the dynamic mechanical experiment, thus allowing both phases to be observed. This phenomenon has also been noted in polyethylene blown films produced under various processing conditions [15].

To further support the aforementioned arguments we should consider the excellent work of Kaplan [16] describing the structure-property relationships in two-phased systems. He defines a compatibility number which is related to the experimental probe size and the size of domains within the multiphase structure. With regards to dynamic mechanical techniques, the probe size is such that for incompatible systems each of the phases is identified giving multiple loss peaks and well defined steps in the storage modulus data. At the other end of the scale, i.e. compatible materials, the probe size extends over both phases resulting in a single loss peak and one step in the storage modulus. For the semi-compatible scenario a broadened modulus curve is observed, analogous to what we observe with the Biopol^{TM} copolymers. The amount of broadening will be indicative of the degree of the distribution of the domain sizes being probed. This, therefore, will alter with the nature of the amorphous/crystalline interface created by the processing conditions. It could be concluded that the so-called texture of the morphology in the interfacial region, as examined by dynamic mechanical techniques, is as a consequence of a distribution of domain sizes.

3.3. Dielectric spectroscopy; low temperature process

Fig. 5 shows an example of the dielectric spectra for an extruded film of D400G (8% HV) at temperatures ranging from 0°C to 30°C. This general shape was exemplified by the compression moulded sample of D400G and also the extruded/compression moulded films of D600G. From previously published data this process is synonymous with the glass transition (T_g) of the amorphous HB/HV moieties. The spectra are very broad (width at half-height of c.a. 4 decades

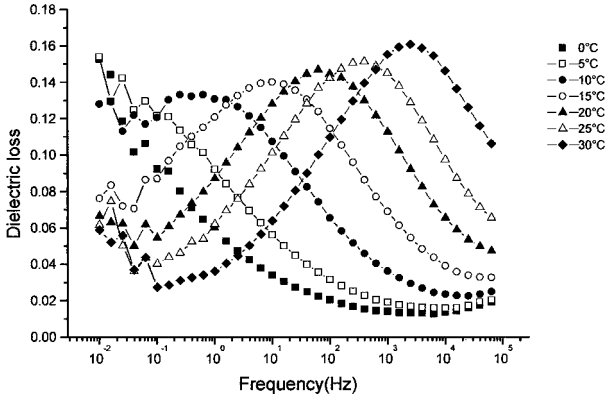

Figure 5 Example of dielectric loss spectrum from 0°C to 30°C for the extruded D400G (8%HV) copolymer.

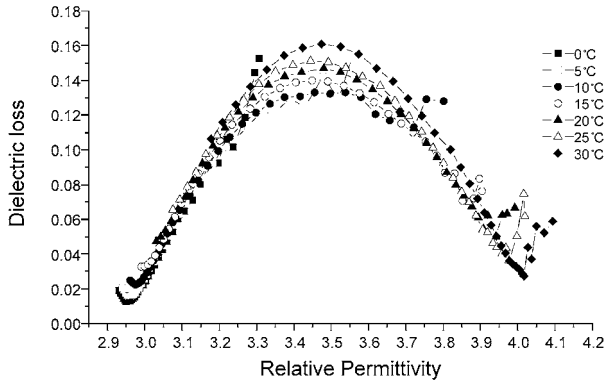

Figure 6 Cole-Cole representation of extruded D400G (8%HV) copolymer.

of frequency) giving the first indication of the large distribution of relaxation times for this process.

Further analysis of the data can be obtained via the Cole-Cole plots [17] (Fig. 6). Utilising the Havriliak-Negami (H-N) [18] approach we are able to evaluate the oscillator strength (ε_0-ε_∞), the relaxation time (τ) and the distribution parameters (α and β). These data are highlighted in Table II.

Using the relaxation time as a function of temperature from the H-N analysis (Fig. 7) we can obtain an activation energy (E_a) for the process (Table II). The most significant observation from the data listed

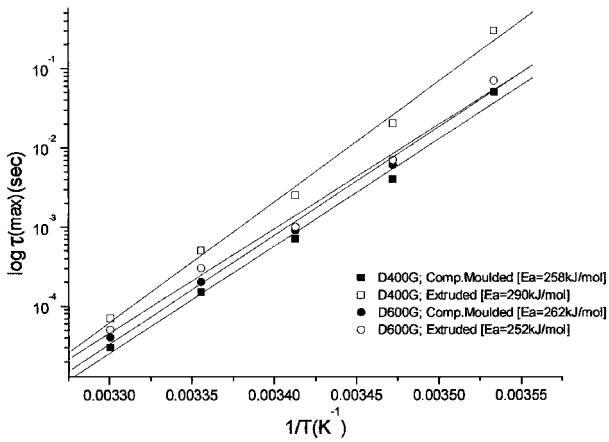

Figure 7 Activation energy calculations based on relaxation times (τ) obtained from Havriliak-Negami analysis.

TABLE II Dielectric parameters evaluated from the Havriliak-Negami analysis of compression moulded and extruded films

Temp(°C)	ε_0-ε_∞	τ(s)	α	β	E_a(kJ·mol^{-1})
D400G(8% HV); Compression moulded					
10	0.87	$5*10^{-2}$	0.32	1	258
15	0.87	$4*10^{-3}$	0.34	1	
20	0.87	$7*10^{-4}$	0.35	1	
25	0.87	$1.5*10^{-4}$	0.36	1	
30	0.87	$3*10^{-5}$	0.375	1	
D400G(8% HV); Extruded					
10	1.05	$3*10^{-1}$	0.32	1	290
15	1.05	$2*10^{-2}$	0.33	1	
20	1.05	$2.5*10^{-3}$	0.345	1	
25	1.05	$5*10^{-4}$	0.355	1	
30	1.05	$7*10^{-5}$	0.375	1	
D600G(12% HV); Compression moulded					
10	0.98	$7*10^{-2}$	0.34	1	262
15	0.98	$6*10^{-3}$	0.345	1	
20	0.98	$9*10^{-4}$	0.355	1	
25	0.99	$2*10^{-4}$	0.36	1	
30	1	$4*10^{-5}$	0.375	1	
D600G(12% HV); Extruded					
10	1.33	$7*10^{-2}$	0.34	1	252
15	1.33	$7*10^{-3}$	0.355	1	
20	1.33	$1*10^{-3}$	0.365	1	
25	1.31	$3*10^{-4}$	0.38	1	
30	1.31	$5*10^{-5}$	0.393	1	

in Table II is the effect of the processing conditions on the oscillator strength. Since this parameter is effectively a measure of the number of dipoles taking part in the relaxation process, it is clear that the extruded material, for both the 8%HV and 12%HV containing copolymers, is significantly different from its compression moulded analogue. In all other aspects the data are relatively constant. There are subtle differences in the apparent activation energies, but more significantly, there appears to be no change in the distribution parameters. This leads to the conclusion that the process under investigation is identical for both processing conditions. Both the energetics and the distribution of processes are unaffected by the copolymer composition or processing conditions. The change in oscillator strength as a function of composition is as we would expect. It is known that the increase in HV content in the copolymer reduces melting temperature and crystallinity. The greater amorphous content, therefore, will lead to a concomitant rise in oscillator strength.

However, together with the DSC data, we have to explain the massive discrepancy between the oscillator strengths as a function of the processing conditions. The DSC data have highlighted the fact that the crystalline/amorphous ratio is relatively insensitive to the processing conditions. However, the change in oscillator strength on going from the extruded (more amorphous) to compression moulded materials is 17% for D400G and almost 26% for D600G. Crude calculations based on the crystalline/amorphous ratios from Table I would suggest that the change in oscillator strength, if it were due to crystallisation of parts of the amorphous phase, would result in an increased crystallinity of 7% for the D400G and 13% for the D600G, on going from extruded to compression moulded parts.

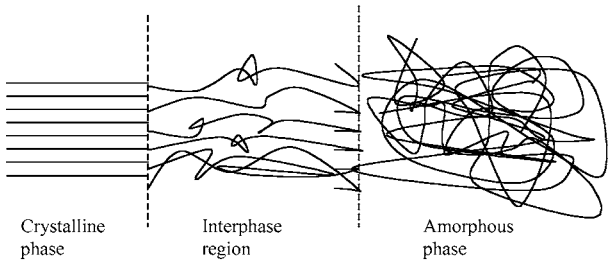

Figure 8 Schematic of the morphology of Biopol^{TM} systems.

To what, then, do we attribute these observations? De Koning *et al.* [2] have argued that the severe embrittlement of moulded PHB should be the result of secondary crystallisation. The DSC data do not uphold this hypothesis. Further, they have maintained that storage of PHB is accompanied by a significant increase in density, at a magnitude greater than that which would be expected for, say a physical ageing process. From the dielectric data, we would envisage a change in the morphology to be responsible for the observations. It is clear from the H-N analysis that the 'pure' amorphous regions are entirely similar, irrespective of composition and processing conditions. The crystalline region, as highlighted by the DSC data, again shows no significant effect of processing. What, therefore, remains, is the interphase (Fig. 8). There appears no doubt that the morphology of the interphase in the compression moulded and extruded samples are quite different. Indeed, de Koning *et al.* [2] allude to this by inferring that the secondary relaxation they are proposing tightly constrains the amorphous phase.

3.4. Dielectric spectroscopy; high temperature process

It is well known in heterogeneous polymer systems such as copolymers and blends that charge build-up at boundaries between two phases of differing conductivities and permittivities can lead to additional dielectric loss processes [19]. These Maxwell-Wagner-Sillars (MWS) processes, due to their inherent dependence on conductivity, tend to occur at low frequency and higher temperature than the glass transition relaxation. Figs 9

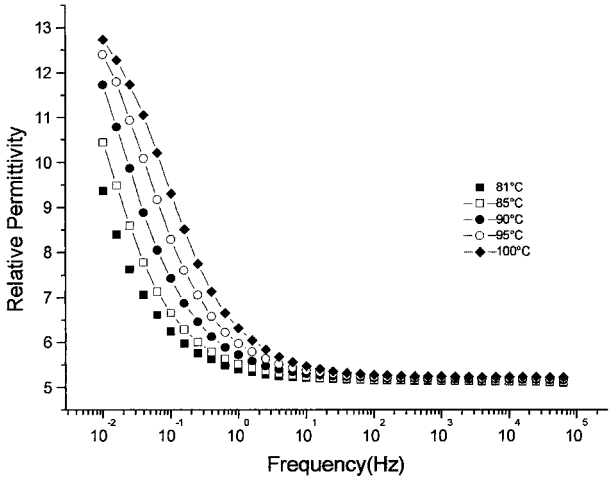

Figure 9 Permittivity as a function of frequency for extruded D400G (8%HV) copolymer from 81°C to 100°C.

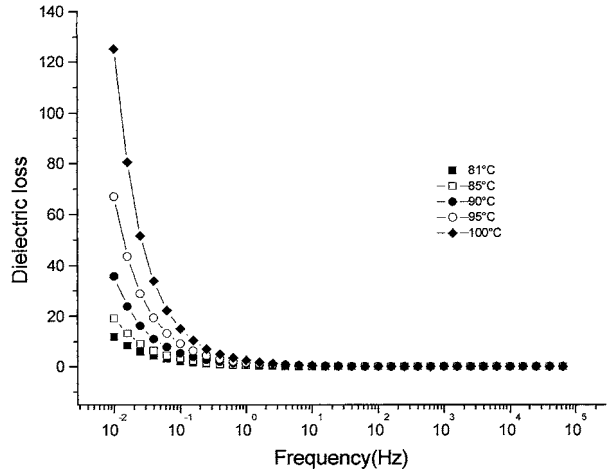

Figure 10 Dielectric loss as a function of frequency for extruded D400G (8%HV) copolymer from 81°C to 100°C.

and 10 highlight the permittivity and loss for the extruded sample of D400G (8%HV). The data clearly show that at low frequencies there is a rapid increase in both the permittivity and loss. If the process is associated with conduction an alternative methodology for representing the dielectric properties is to utilise the complex inverse permittivity or electrical modulus [20, 21]:

$$M^*(\omega) = 1/\varepsilon^*(\omega) = M'(\omega) + iM''(\omega) \quad (1)$$

$$M' = \frac{\varepsilon'}{(\varepsilon')^2 + (\varepsilon'')^2}; \quad M'' = \frac{\varepsilon''}{(\varepsilon')^2 + (\varepsilon'')^2} \quad (2)$$

Applying this to the sample of D400G (8%HV) leads to Fig. 11. We can clearly see that a process emerges, moving to higher frequencies as a function of temperature. This experiment was repeated for a sample of D600G (12%HV). An estimation of the energetics of the processes was undertaken by constructing Arrhenius plots of log f_{max} as a function of the reciprocal absolute temperature (Fig. 12). The apparent activation energies were calculated as 153 kJ/mol and 130 kJ/mol for the D400G and D600G respectively. These values are much lower than those quoted in Table II for the T_g process but are more representative of a conduction process. Further, they are in good agreement with data published for the PHB homopolymer [5]. Although there is a slight difference in the activation energies of the copolymers, the effective 'transition temperatures', at constant frequency, are markedly different. Theories for the MWS process show that the conductivity, volume fraction and also the shape of the component phases play a defining role in determining the frequency, or more accurately, the relaxation time. With regards to the copolymers under investigation, we speculate that the changes in the nature of the interphase will affect the conductivity and hence, the relaxation time.

3.5. Thermally stimulated discharge (TSD)

The poling conditions, with respect to poling temperature, were based on the temperatures at which the high temperature, imaginary modulus peaks were located.

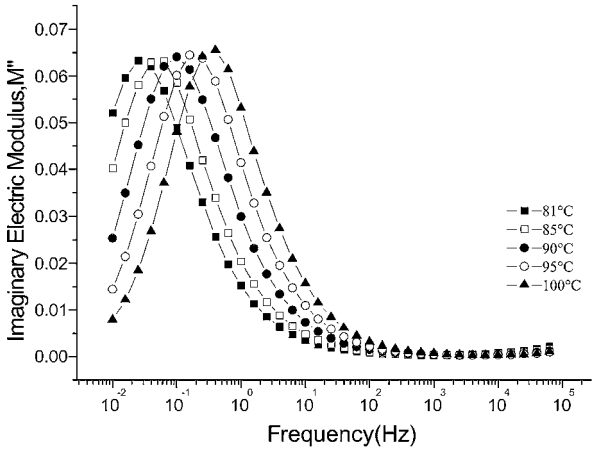

(a)

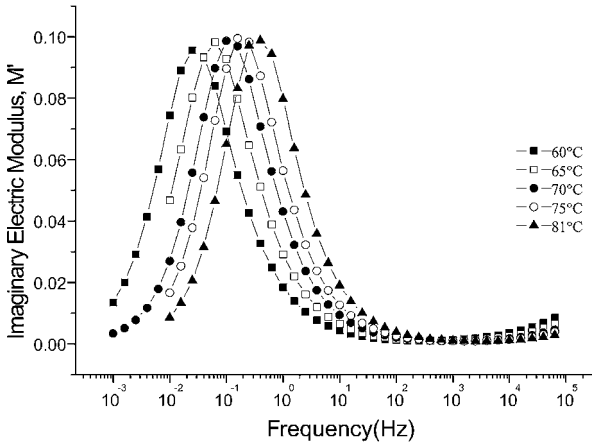

(b)

Figure 11 (a) Imaginary electric modulus as a function of frequency for extruded D400G (8%HV) copolymer from 81°C to 100°C. (b) Imaginary electric modulus as a function of frequency for extruded D600G (12%HV) copolymer from 81°C to 100°C.

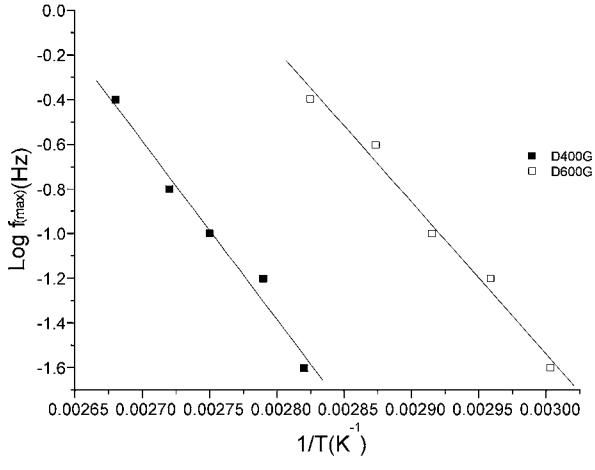

Figure 12 Arrhenius plots of log $f_{(max)}$ versus reciprocal absolute temperature for the imaginary electric modulus of D400G (8%HV) and D600G (12%HV) copolymers.

For both the D400G and D600G systems we chose a poling temperature (T_p) of 80°C and a depole temperature (T_d) of −50°C. A voltage (V) of 1 kV was applied. The final discharge current was measured using a constant ramp rate of 3°C/minute. The TSD spectra for the compression moulded and extruded parts are highlighted in Fig. 13a and b.

As was expected the T_g process, highlighted in both the DMTA and low temperature dielectric spectroscopy, is clearly evident in all the samples, occurring around 15°C–20°C. The activation energy can be determined by the method of Grossweiner [22] using:

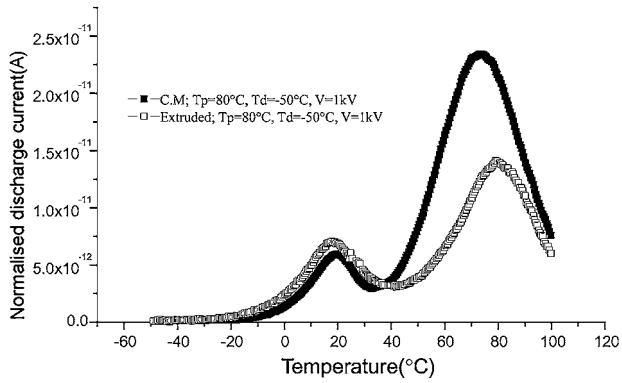

(a)

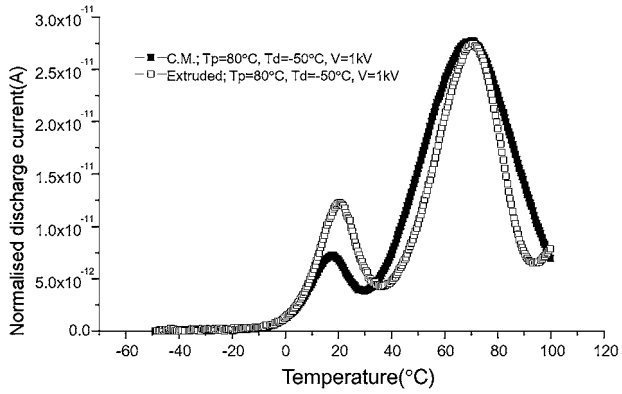

(b)

Figure 13 (a) Normalised TSD spectra for the D400G (8%HV) copolymer as a function of processing conditions. (b) Normalised TSD spectra for the D600G (12%HV) copolymer as a function of processing conditions.

$$E_a = \frac{1.51kT_mT_{1/2}}{T_m - T_{1/2}} \quad (4)$$

Where T_m is the temperature at peak maximum, $T_{1/2}$ is the temperature corresponding to the half height of the peak on the low temperature side and k is the Boltzmann constant. The calculated activation energies for the T_g process are listed in Table III.

The interpretation of TSD spectra is exceedingly complicated. Many authors have analysed spectra in an attempt to correlate their findings with, say, equivalent a.c.dielectric data, with varying degrees of success. However, Hedvig [23] has pointed out that in the case where the temperature dependence of the oscillator

TABLE III Calculated parameters from the TSD spectra of compression moulded and extruded films

		E_a (kJ/mol) [TSD]		ε_0-ε_∞ [TSD]	
Sample	Processing	T_g peak	MWS peak	T_g peak	MWS peak
D400G	Compression moulded	88	74	1.26	8.6
D400G	Extruded	77	83	2.09	4.9
D600G	Compression moulded	110	62	1.15	11
D600G	Extruded	112	82	2.24	8.3

strength (ε_0-ε_∞) is negligible; then, and only then, the frequency scale can be transformed into the temperature scale and vice versa. His contention is that TSD is solely a qualitative method for detecting dielectric transitions.

From the point of view of this study we accept Hedvig's basic point, but calculation of parameters from the TSD data can serve to semi-quantify differences which are then used to infer changes in the internal structure and morphology of complex polymer systems. The calculated parameters for the T_g process in Table III serve to exemplify this approach. The activation energies are very different from those observed in the a.c.dielectric experiment (Table II). To try to understand these large discrepancies we have to understand that although the two techniques are based on an electrical perturbation and subsequent response, there are inherent differences both in the molecular mechanisms and data analysis. In a study of epoxy systems Daly *et al*. [24] have maintained that one possible origin of the TSD peak, assumed to be the glass transition, is as a consequence of short-scale migration of charge assisted by local motions of the polymer chain. The fact that the mechanism includes the role of the conductivity will hence result in a lower activation energy than a purely dipolar process. Also, the H-N data analysis contains distribution parameters describing the large variation of dipolar environments. The theories, however, considered for the TSD data do not include such distributions, being based simply on a single, discrete process.

Equation 5 can be used to calculate the oscillator strength of the relaxation process [25]:

$$\varepsilon_0 - \varepsilon_\infty = \frac{Q}{E.A.\varepsilon_0} \tag{5}$$

where, Q is the total charge (area under the TSD peak/heating rate), E is the electric field, A is the electrode area and ε_0 is the permittivity of free space. Values for the copolymers are given in Table III. The data for the compression moulded parts seem in good agreement with the values of Table II, however, the extruded materials are certainly not comparable. Nonetheless, it gives a qualitative picture of the differences which the two processing modes imparts to the samples.

The higher temperature peak is no less complex. However, its very existence in the TSD experiment is of great interest. It serves to suggest that the complex modulus representation used earlier is valid and that there is, indeed, another relaxation process ongoing in the copolymers. As with the T_g process we have calculated the activation energies and oscillator strengths (Table III). The activation energies are not too dissimilar to the T_g values again suggesting a mechanism based on a conduction induced process [5]. The oscillator strengths are much higher than the T_g peak which is as expected for an MWS type relaxation [26].

Like the lower temperature peak the differences with respect to the processing conditions are manifest. From a numerical standpoint, with respect to both peaks, we see the relationship: ε_0-ε_∞(compression moulded) $<\varepsilon_0$-ε_∞(extruded), for the T_g peak, whereas ε_0-ε_∞ (compression moulded)$>$ ε_0-ε_∞(extruded) for the MWS process. As previously discussed we are loath to make too much of the calculated values, but they are no doubt significant and highlight the difference in the nature of the subtle structure produced in the copolymers via the processing step.

In order to elucidate the origin of the high temperature peak in Biopol copolymers we can consider previous studies on another semi-crystalline system, viz. polyethylene. Bericat [27] *et al*. have observed a very broad, post T_g transition in low density polyethylene which has been assigned to different modes of motion by molecular segments constituting the folds and/or ciliary parts of lamellae. Other work by Motori [28] and co-workers on the effect of ageing on crosslinked polyethylene has also identified a high temperature process by TSD. Their quoted peak temperatures and activation energies agree favourably with those in Table III and moreover, are recorded on samples involved in an ageing study. As we have previously intimated, they observe that the activation energies are consistent with a conduction process, i.e. motion of charge carriers, and have ascribed the relaxation to charge polarisation related to melting of the crystalline region of the polymer.

The fact that the temperature of the peaks for the Biopol systems and polyethylene are so similar, together with the fact that no DSC evidence is forthcoming as to any exothermic/endothermic processes in this temperature range, further enhances the hypothesis that this process has its origin in a morphologically induced phenomenon.

4. Conclusions

The amorphous and crystalline regions in Biopol copolymers can be well defined by DMTA, dielectric spectroscopy and DSC methods. It has been highlighted that the processing step causes no change to the pure crystalline phase in terms of the melting temperature and level of crystallinity. Dielectric studies on the T_g process further emphasise that the processing conditions do not affect the overall molecular motion dynamics as viewed via the activation energies and distribution parameters. The methodology of the complex modulus representation allows us to highlight a relaxation above the T_g which has all the characteristics of a MWS process. TSD studies confirm the existence of a post T_g relaxation whose attributes are consistent with a process derived from conductivity effects. Changes as a consequence of processing variations are interpreted as being due to morphological reorganisation in the interfacial regions. Further work is ongoing to study these phenomena using a broader range a samples with better defined ageing characteristics.

Acknowledgements

R. C and J. H. D. acknowledge the EPSRC for funding during the course of this work.

References

1. T. HAMMOND and J. J. LIGGAT, in "Degradable Polymers," edited by G. Scott and D. Gilead (Chapman & Hall, London, 1995) p. 88.

2. G. J. M. DE KONING and P. J. LEMSTRA, *Polymer* **34** (1993) 4089.
3. G. J. M. DE KONING, A. H. C. SCHEEREN, P. J. LEMSTRA, M. PEETERS and H. REYNAARS, *ibid.* **35** (1994) 4598.
4. F. BIDDLESTONE, A. HARRIS, J. N. HAY and T. HAMMOND, *Polymer International* **39** (1996) 221.
5. G. J. PRATT and M. J. A. SMITH, *Eur. Polym. J.* **33** (1997) 857.
6. I. SICS, V. TUPUREINA, M. KALINS, T. A. EZQUERRA and F. J. BALTA-CALLEJA, *J. Macromol. Sci. Phys.* **B37** (1998) 851.
7. G. R. SAAD, A. A. MANSOUR and A. H. HAMED, *Polymer* **38** (1997) 4091.
8. J. VAN TURNHOUT, in "Thermally Stimulated Discharge of Polymer Electrets" (Elsevier, Amsterdam, 1980).
9. J. H. DALY, M. J. GUEST, D. HAYWARD and R. A. PETHRICK, *J. Mater. Sci. Lett.* **10** (1991) 441.
10. R. J. RULE and J. J. LIGGAT, *Polymer* **36** (1995) 3831.
11. M. SANCHEZ-CUESTA, J. MARTINEZ-SALAZAR, P. A. BARKER and P. J. BARHAM, *J. Mater. Sci.* **27** (1992) 5335.
12. M. J. GUEST and J. H. DALY, *Eur. Polym. J.* **26** (1990) 603.
13. M. J. GUEST, J. H.DALY and L. AERTS, in Polymer Blends: Science, Technology and Applications; Int.Conf., Egham, U.K. 1988.
14. D. QUINTENS, G. GROENINCKX, M. J. GUEST and L. AERTS, *Polym. Eng. Sci.* **31** (1991) 1207.
15. J. H. DALY, *Eur. Polym. J.* **26** (1990) 933.
16. D. S. KAPLAN, *J. Appl. Polym. Sci.* **20** (1976) 2615.
17. S. H. COLE and R. H. COLE, *J. Chem. Phys.* **9** (1941) 341.
18. S. HAVRILIAK and S. NEGAMI, *J. Polym. Sci. C* **14** (1966) 99.
19. L. K. H. VAN BEEK, *Progress in Dielectrics* **7** (1967) 69.
20. A. A. BAKR, A. M. NORTH and G. KOSSMEHL, *Eur. Polym. J.* **13** (1977) 799.
21. M. TABELLOUT, H. RANDRIANANTOANDRO, J. R. EMERY, D. DURRAND, D. HAYWARD and R. A. PETHRICK, *Polymer* **36** (1995) 4547.
22. L. I. GROSSWEINER, *J. Appl. Phys.* **24** (1953) 1306.
23. P. HEDVIG, in "Applied Polymer Analysis and Characterisation," Vol. 2, edited by J. Mitchell Jr. (Hanser, Munich, 1991).
24. J. H. DALY, K. JEFFREY, D. HAYWARD, R. A. PETHRICK and P. WILFORD, *J. Mater. Sci.* **28** (1993) 2028.
25. J. VAN TURNHOUT, *Polym. J.* **2** (1973) 191.
26. J. H. DALY, M. J. GUEST, D. HAYWARD and R. A. PETHRICK, *J. Mater. Sci. Lett.* **11** (1992) 1271.
27. P. BERTICAT, B. AI, H. T. GIAM, DCHATAIN and C. LACABANNE, *Makromol. Chem.* **177** (1976) 1583.
28. A. MOTORI, G. C. MONTANARI and S. GUBANSKI, *J. Appl. Polym. Sci.* **59** (1996) 1715.

Received 29 November 1999
and accepted 15 January 2001